Digital Signal Processing **9,** 162–177 (1999)
Article ID dspr.1999.0341, available online at http://www.idealibrary.com on IDEAL®

Stochastic Resonance and Optimal Detection of Pulse Trains by Threshold Devices

François Chapeau-Blondeau

Laboratoire d'Ingénierie des Systèmes Automatisés (LISA),
Université d'Angers, 62 avenue Notre Dame du Lac, 49000 Angers, France
E-mail: chapeau@univ-angers.fr

Chapeau-Blondeau, François, Stochastic Resonance and Optimal Detection of Pulse Trains by Threshold Devices, *Digital Signal Processing* **9** (1999), 162–177.

The nonlinear detection by a threshold device of a periodic train of soliton-like pulses embedded in arbitrarily distributed white noise is studied. A theoretical model is developed which provides expressions for the signal-to-noise ratio at the output of the detector and for the input–output gain in signal-to-noise ratio. We analyze the properties and conditions of optimality for these quantities as functions of the parameters of the process. Especially, specific nonlinear properties not shared by linear devices are established, among which are the possibility of an input–output amplification of the signal-to-noise ratio and the demonstration that through nonlinear coupling the noise can be beneficial to the signal detection and that adding noise may result in improved performance via a mechanism known as stochastic resonance.

1. INTRODUCTION

Signal processing, especially at low levels where a signal is to be recovered out of the noise, relies heavily on linear devices, involving linear sensors followed by linear filtering. Linear techniques are specially interesting because they usually allow a thorough theoretical treatment, providing extensive control over the processes [1]. Yet linear techniques also come with inherent limitations, and one may turn to nonlinear techniques or devices in order to gain additional properties. In the nonlinear domain, no comparable general theory is available to guide the design and analysis of signal-processing devices. The exploration and exploitation of nonlinear processes is still in its infancy, and certainly many interesting and useful nonlinear properties remain to be discovered and mastered [2, 3].

In a specific context here, we develop an analysis of a nonlinear process concerning the detection of signal in noise. We show the possibility of

1051-2004/99 $30.00

interesting and powerful "nonlinear" performances not present in linear devices. Especially, we demonstrate that through nonlinear coupling, the noise can be beneficial to the signal detection and that adding noise may result in improved performance via a mechanism known as stochastic resonance [4].

We consider a periodic signal $s(t)$ consisting of a rectangular pulse of the amplitude $A > 0$ and duration T, repeated at the period $T_s > T$; i.e., $s(t) = A$ for $t \in [0, T < T_s[$ and $s(t) = 0$ elsewhere in the period T_s. This signal $s(t)$ is corrupted additively by a stationary white noise $\eta(t)$ with probability density function $f_\eta(u)$ and cumulative distribution function $F_\eta(u) = \int_{-\infty}^{u} f_\eta(u')du'$.

The signal $s(t)$ is seen here as a model for different types of physical signals carrying information in the form of discrete pulses. For example, this can be the case of trains of neural action potentials or of neural postsynaptic potentials [5]. In such neural trains, the "firing" period T_s can code for the intensity of a stationary stimulus. Also, the periodic train $s(t)$ can represent a high-frequency carrier which can carry useful information through modulation by a low-frequency (quasi-static) message. Another embodiment would be a train of solitons in a nonlinear setting [6].

We further consider that the signal-plus-noise mixture $s(t) + \eta(t)$ is received by a threshold detector producing the response $y(t) = g[s(t) + \eta(t)]$ with

$$g(u) = \begin{cases} 0 & \text{for } u \leq \theta, \\ 1 & \text{for } u > 0. \end{cases} \tag{1}$$

Equation (1) can be seen as a simple model for the essential nonlinearity in a neuron response (i.e., a threshold nonlinearity). It can also represent the response of a bistable optical device, or of many other devices (e.g., electronic) [7]. Whatever its physical implementation, we shall demonstrate that the nonlinear response of Eq. (1) possesses very interesting and unusual properties (not shared by linear detectors) for efficient recovery of the information-carrying pulse train $s(t)$ out of the signal-plus-noise mixture $s(t) + \eta(t)$.

2. FREQUENCY-DOMAIN ANALYSIS

A signal-to-noise ratio (SNR) in the frequency domain will now be evaluated, both at the input and at the output of the threshold detector, through an application of the theory proposed in [8].

At the input, the power spectral density of the signal-plus-noise mixture $s(t) + \eta(t)$ is formed by spectral lines (Dirac delta functions) at the harmonics n/T_s contributed by the T_s-periodic input $s(t)$, emerging out of a broadband continuous background contributed by the white noise input $\eta(t)$. The power contained in the spectral line at frequency n/T_s is $|S_n|^2$, with the order n Fourier coefficient of the pulse train $s(t)$ given by

$$S_n = A \frac{T}{T_s} \operatorname{sinc}\left(n\pi \frac{T}{T_s}\right) \exp\left(-in\pi \frac{T}{T_s}\right). \tag{2}$$

In the same way, at the output, the power spectral density is formed by spectral lines at the harmonics n/T_s originating in the T_s-periodic input $s(t)$, emerging out of a broadband continuous background originating in the white noise $\eta(t)$. The power contained in the spectral line at frequency n/T_s is given [8] by $|\overline{Y}_n|^2$, where $\overline{Y}_n$ is the order n Fourier coefficient of the T_s-periodic non-stationary output mean $E[y(t)]$,

$$\overline{Y}_n = \frac{1}{T_s}\int_0^{T_s} E[y(t)] \exp\left(-in\,\frac{2\pi}{T_s}\,t\right) dt, \tag{3}$$

with the mean $E[y(t)]$ at a fixed time t expressable as

$$E[y(t)] = 1 \times \Pr[s(t) + \eta(t) > \theta] = 1 - F_\eta[\theta - s(t)]. \tag{4}$$

For $s(t)$ our train of rectangular pulses, Eqs. (3)–(4) result in

$$\overline{Y}_n = [F_\eta(\theta) - F_\eta(\theta - A)]\,\frac{T}{T_s}\,\mathrm{sinc}\left(n\pi\,\frac{T}{T_s}\right)\exp\left(-in\pi\,\frac{T}{T_s}\right). \tag{5}$$

We now possess explicit expressions for the coherent powers located in spectral lines at n/T_s in both the input and output power spectral densities. We shall now evaluate the magnitude of the broadband noise background out of which these spectral lines emerge, both at the input and at the output. For this purpose, to avoid artificial difficulties stemming from the idealized character of a white noise (infinite variance and zero correlation duration) we shall move to a discrete-time description. The time scale is discretized with a step $\Delta t \ll T < T_s$. The white noise is implemented with the discrete-time sequence $\eta(t = j\Delta t)$ of independent values identically distributed according to the density $f_\eta(u)$ with the finite variance σ_η^2. The correlation duration of the discrete white noise is no larger than Δt, and the product $\sigma_\eta^2\Delta t$ is fixed and finite and measures the power spectral density of the white noise.

In the input power spectral density, the noise background thus has the constant amplitude $\sigma_\eta^2\Delta t$. The power contained in this noise background in a small frequency band ΔB around the harmonic n/T_s is simply $\sigma_\eta^2\Delta t\Delta B$. A classical definition of the signal-to-noise ratio [8], at frequency n/T_s, follows as the ratio of the power $|S_n|^2$ contained in the spectral line to the power contained in the noise background in the small frequency band ΔB around n/T_s. This results in the expression of the input SNR as

$$R_{\mathrm{in}}\left(\frac{n}{T_s}\right) = \frac{|S_n|^2}{\sigma_\eta^2\Delta t\Delta B}\,. \tag{6}$$

In a similar way, the magnitude of the noise background in the output power spectral density is given [8] by $\overline{\mathrm{var}(y)}\Delta t$, with the stationarized output variance

$$\overline{\mathrm{var}(y)} = \frac{1}{T_s}\int_0^{T_s} \mathrm{var}[y(t)]dt, \tag{7}$$

expressable from the nonstationary variance var[$y(t)$] at a fixed time t:

$$\text{var}[y(t)] = E[y^2(t)] - E^2[y(t)] = F_\eta[\theta - s(t)]\,[1 - F_\eta[\theta - s(t)]]. \tag{8}$$

And for $s(t)$ our train of rectangular pulses, Eqs. (7)–(8), result in

$$\overline{\text{var}(y)} = \frac{T}{T_s} F_\eta(\theta - A)\,[1 - F_\eta(\theta - A)] + \left(1 - \frac{T}{T_s}\right) F_\eta(\theta)[1 - F_\eta(\theta)]. \tag{9}$$

The output SNR, defined in the same way as the input SNR, follows as

$$R_{\text{out}}\left(\frac{n}{T_s}\right) = \frac{|\overline{Y}_n|^2}{\overline{\text{var}(y)}\Delta t \Delta B}, \tag{10}$$

which, thanks to Eqs. (5) and (9), is

$$R_{\text{out}}\left(\frac{n}{T_s}\right) = \frac{[F_\eta(\theta) - F_\eta(\theta - A)]^2}{\dfrac{T}{T_s}F_\eta(\theta - A)\,[1 - F_\eta(\theta - A)] + \left(1 - \dfrac{T}{T_s}\right) F_\eta(\theta)[1 - F_\eta(\theta)]} \times \frac{\left(\dfrac{T}{T_s}\right)^2 \text{sinc}^2\left(n\pi \dfrac{T}{T_s}\right)}{\Delta t \Delta B}. \tag{11}$$

Another quantity of interest [9], to characterize the operation of the threshold detector, is the input–output gain $G_{\text{SNR}} = R_{\text{out}}/R_{\text{in}}$ for the SNR, whose expression is found to be the same at any harmonic n/T_s, and follows as

$$G_{\text{SNR}} = \frac{[F_\eta(\theta) - F_\eta(\theta - A)]^2\, \sigma_\eta^2/A^2}{\dfrac{T}{T_s}F_\eta(\theta - A)[1 - F_\eta(\theta - A)] + \left(1 - \dfrac{T}{T_s}\right) F_\eta(\theta)[1 - F_\eta(\theta)]}. \tag{12}$$

Without loss of generality, we can take $A = 1$ for the unit of amplitude, in which both θ and σ_η will now be expressed. The quantity G_{SNR} of Eq. (12) and, also, the quantity R_{out} of Eq. (11) at a given harmonic n/T_s, are taken as measures of the performance of the threshold detector. We shall now analyze them and exhibit some interesting properties. Especially, R_{out} and G_{SNR} are both functions of three important parameters characterizing the transmission process: the pulse duration T/T_s, the threshold θ, and the noise rms amplitude σ_η (via F_η). We shall study these dependencies and examine the optimality conditions on T/T_s, θ, and, also, σ_η, in order to maximize R_{out} or G_{SNR} in different situations.

3. MAXIMIZATION OF THE OUTPUT SNR

We assume first that the type of noise distribution (Gaussian, for example) and its variance σ_η^2 are fixed, and we study the variations of R_{out} at the fundamental $1/T_s$, as a function of T/T_s and θ.

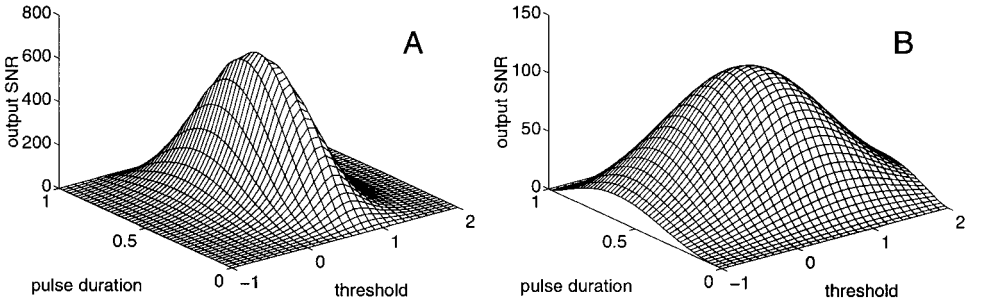

FIG. 1. Output SNR $R_{out}(1/T_s)$ from Eq. (11) as a function of the pulse duration T/T_s and the threshold θ, when the input white noise $\eta(t)$ is zero-mean Gaussian with rms amplitude $\sigma_\eta = 0.4$ (panel A) and $\sigma_\eta = 0.8$ (panel B).

Figure 1 shows two typical evolutions of R_{out}, as a function of T/T_s and θ when $\eta(t)$ is a zero-mean Gaussian noise, and with the product $\Delta t \Delta B$ in Eqs. (11) and (10) chosen to be 10^{-3} (we shall stick to this value throughout the paper).

In the case of the Gaussian $\eta(t)$ of Fig. 1, the cumulative distribution is $F_\eta(u) = 0.5 + 0.5\ \mathrm{erf}[u/(\sqrt{2}\sigma_\eta)]$. If both T/T_s and θ are free adjustable parameters, the optimization of R_{out} in Eq. (11) shows that the absolute maximum accessible for R_{out} is reached when $(T/T_s, \theta) = (0.5, 0.5)$ for any noise rms amplitude σ_η. If, on the contrary, a fixed value for $T/T_s \neq 0.5$ (or, respectively, for $\theta \neq 0.5$) is imposed by the transmission process, the optimal value of the complementary parameter θ (or T/T_s) maximizing R_{out} will differ from the value at the absolute maximum and will depend on σ_η, as is seen in Fig. 1. To illustrate this property, Fig. 2A shows the values of the threshold θ (at different noise levels σ_η) maximizing R_{out} when the value of T/T_s is fixed. Figure

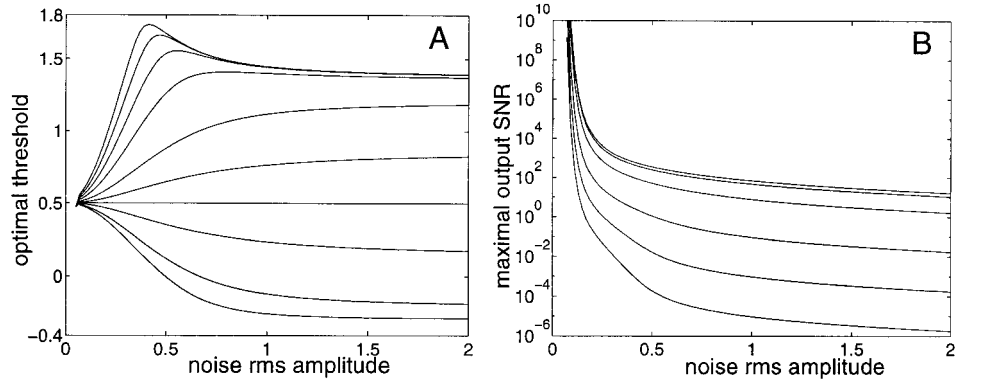

FIG. 2. At a fixed pulse duration T/T_s, optimal threshold θ, maximizing the output SNR $R_{out}(1/T_s)$ of Eq. (11) (panel A) and maximum value of $R_{out}(1/T_s)$ at the optimal threshold (panel B), as a function of the rms amplitude σ_η of the zero-mean Gaussian noise $\eta(t)$. In panel A, from the lowest to the upper curve, $T/T_s = 0.95, 0.9, 0.7, 0.5, 0.3, 0.1, 10^{-2}, 10^{-3}, 10^{-4}$, and 10^{-6}. In panel B, from the upper to the lowest curve, $T/T_s = 0.5, 0.3, 0.1, 10^{-2}, 10^{-3}$, and 10^{-4}, in addition, a curve at $T/T_s = 0.7$ is superimposed to the curve at $T/T_s = 0.3$, and a curve at $T/T_s = 0.9$ is superimposed to the curve at $T/T_s = 0.1$, illustrating the nonmonotonic influence of T/T_s.

2B shows the corresponding maximum value of R_{out}, which reaches its overall maximum when $T/T_s = 0.5$ in the Gaussian case.

Optimality conditions for the threshold detector operating at a fixed T/T_s, which are not intuitive in the first place, are revealed by the analysis illustrated in Fig. 2A. Conditions exist (for sufficient noise levels), where the optimal value of the threshold θ is above 1, i.e. above the magnitude of the coherent pulses to be detected which become subliminal. Also, in other conditions (for T/T_s sufficiently large), the optimal threshold θ can become negative.

Complementary to Fig. 2 is Fig. 3, which shows the values of the pulse duration T/T_s (at different noise levels σ_η), maximizing R_{out} when the value of θ is fixed, and also, the corresponding maximum value of R_{out} which reaches its overall maximum when $\theta = 0.5$ in this Gaussian case.

An especially interesting property appearing in Fig. 3B, for the threshold detector operating at a fixed θ, is that there exist conditions, at a fixed $\theta > 1$, where the output SNR R_{out} can increase when the input noise rms amplitude σ_η is raised. The same property is also present, at a fixed $\theta > 1$, when the pulse duration T/T_s is fixed at a value differing from its optimum of Fig. 3A, as depicted by Fig. 4.

In the regime with the threshold $\theta < 1$, the input pulses alone are above threshold and able by themselves to trigger transitions in the output $y(t)$. In this case, in the absence of the noise, the output $y(t)$ perfectly reproduces the input train $s(t)$ and the output SNR R_{out} goes to infinity. When the noise level is gradually raised above zero, the output transitions coherent with the input pulses will gradually get polluted by more and more noisy transitions. This entails a monotonic decay of R_{out} with increasing noise level, as is seen in Figs. 3B and 4A when $\theta < 1$.

By contrast, in the regime with $\theta > 1$, the input pulse train $s(t)$ alone is subliminal and unable by itself to trigger transitions in the output $y(t)$. In this

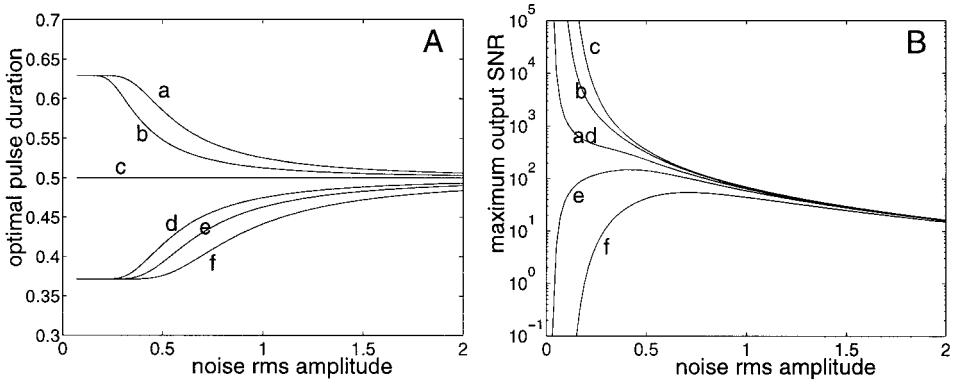

FIG. 3. At a fixed threshold θ, the optimal pulse duration T/T_s maximizing the output SNR $R_{out}(1/T_s)$ of Eq. (11) (panel A), and maximum value of $R_{out}(1/T_s)$ at the optimal pulse duration (panel B), as a function of the rms amplitude σ_η of the zero-mean Gaussian noise $\eta(t)$ with $\theta = 0.1$ (a), $\theta = 0.3$ (b), $\theta = 0.5$ (c), $\theta = 0.9$ (d), $\theta = 1.1$ (e), $\theta = 1.5$ (f). In panel B, the two curves, (a) for $\theta = 0.1$ and (d) for $\theta = 0.9$, are superimposed, illustrating the nonmonotonic influence of θ.

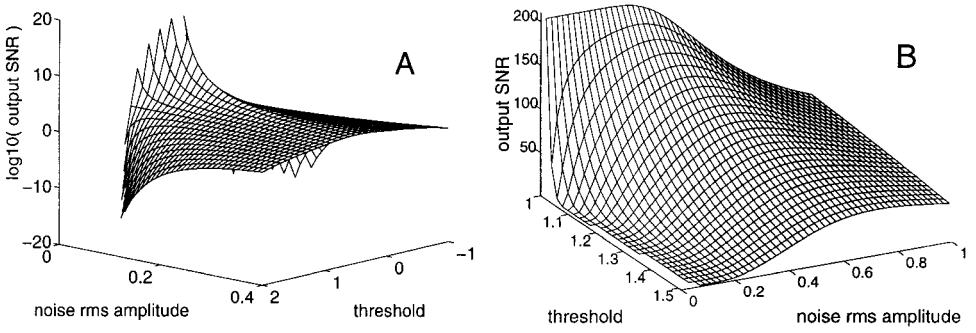

FIG. 4. Output SNR $R_{\text{out}}(1/T_s)$ of Eq. (11) as a function of the threshold θ and of the rms amplitude σ_η of the zero-mean Gaussian noise $\eta(t)$, at a given pulse duration $T/T_s = 0.5$. As σ_η increases, panel A shows both the regime where R_{out} decreases (at $\theta < 1$) and the regime where R_{out} can increase (at $\theta > 1$); panel B is a close-up on this last regime, where R_{out} can be increased when σ_η increases, revealing a form of stochastic resonance.

case, in the absence of the noise, the periodic input $s(t)$ is invisible in the output $y(t)$, and the output SNR R_{out} is zero. When the noise level is gradually raised above zero, a cooperative effect becomes possible in which the noise can assist the coherent input $s(t)$ in overcoming the threshold θ. The result is that output transitions can occur which bear a correlation with the input pulses because their occurrences involve the joint action of the noise and the coherent pulses. As the noise level gets larger, the probability of this favorable outcome first increases, leading to a reinforcement of the correlation of the output with the input pulse train which translates to an increasing output SNR R_{out}. There exists an optimum nonzero noise level, where R_{out} is maximized. Past this optimum, when the noise level is further raised, the output transitions produced by the noise alone, with no assistance from the coherent pulses, grow in importance and gradually destroy the correlation of the output with the coherent pulse train, resulting in the eventual decay of R_{out}. This noise enhancement of the output SNR is visible in Figs. 4B and 3B when $\theta > 1$.

This noise-assisted signal transmission is a form of stochastic resonance. The phenomenon of stochastic resonance was introduced some 15 years ago [10] in a nonlinear system more complicated than our threshold detector of Eq. (1). It was a nonlinear dynamic system (by contrast Eq. (1) rather constitutes a static or memoryless nonlinear system) governed by a bistable potential in which it was shown that the response to a sinusoidal forcing can be improved via noise addition. In this form, the effect of stochastic resonance has been the subject of much elaboration [11, 12, 4]. Only recently has stochastic resonance been reported for simpler nonlinear systems amenable to a general theory and easily implementable as signal processing devices [8, 13, 14]. A stochastic resonant system of the type of Eq. (1) with a calculation of R_{out} and G_{SNR} appeared for the first time in [9], essentially to establish the existence of the stochastic resonance effect. But it is here for the first time that the influences of the parameters of the nonlinear transmission are systematically studied and that the problem of optimizing the transmission in the presence of stochastic

resonance is addressed, especially to determine the conditions maximizing the performance.

The stochastic resonance is revealed here in Figs. 3B and 4 by the nonmonotonic resonant evolution of $R_{out}(1/T_s)$, observed at the first harmonic $1/T_s$. It is to note that, thanks to the form of R_{out} of Eq. (11), resonant evolutions will also exist for $R_{out}(n/T_s)$ at higher order harmonics of n/T_s. Also the conditions of Figs. 3 and 4, especially the Gaussian quality of the noise and the value of T/T_s, are merely illustrative and are not critical for the existence of the stochastic resonance effect with a subliminal input pulse train.

In the regime where $\theta < 1$, the output SNR is maximized at zero noise. In the regime where $\theta > 1$, where stochastic resonance takes place, Eq. (11) shows that the maximum R_{out} is obtained at the same conditions for any harmonic of n/T_s, and Fig. 5A presents the optimal value of the noise rms amplitude σ_η maximizing R_{out} of Eq. (11) for the case of Gaussian noise $\eta(t)$. Figure 5B presents the corresponding maximum R_{out} afforded by the optimal noise level. Figure 5 is a vivid illustration of the stochastic resonance effect, showing that if the threshold detector has to operate at a fixed $\theta > 1$, an optimal nonzero noise level is required to maximize R_{out}. This may lead, in the case of too little noise, to purposely adding more noise in order to maximize the performance.

4. MAXIMIZATION OF THE INPUT–OUTPUT SNR GAIN

We now turn to the analysis of the SNR gain G_{SNR} of Eq. (12) as a function of T/T_s and θ. Figure 6 shows two typical evolutions of G_{SNR} with T/T_s and θ, when $\eta(t)$ is a zero-mean Gaussian noise.

The results of Fig. 6 show that over a definite domain of conditions, it is possible to obtain a SNR gain G_{SNR} larger than unity, i.e. an input–output amplification of the SNR by the nonlinear threshold detector. This is a very important property that cannot be obtained with a linear device, which always

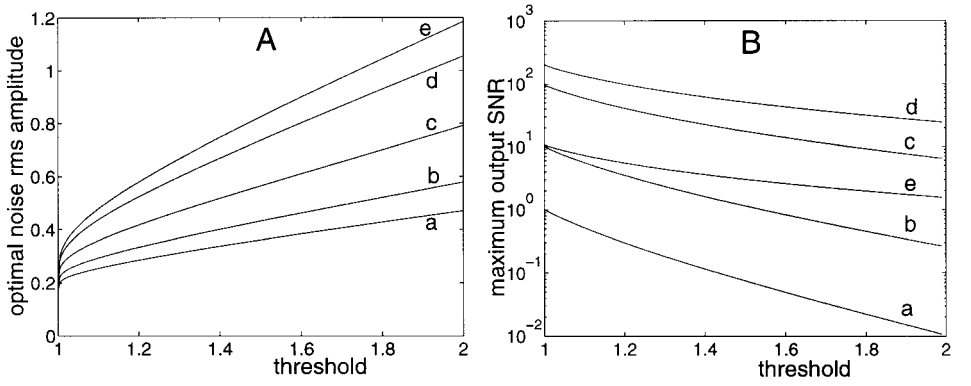

FIG. 5. For a zero-mean Gaussian input noise $\eta(t)$, as a function of the threshold $\theta > 1$, with $T/T_s = 10^{-3}$ (a), 10^{-2} (b), 0.1 (c), 0.5 (d), 0.9 (e). Panel A shows the optimal value of the input noise rms amplitude σ_η maximizing the output SNR R_{out} of Eq. (11). Panel B shows the maximum output SNR $R_{out}(1/T_s)$ at the optimal σ_η (a nonmonotonic influence of T/T_s on R_{out} is visible).

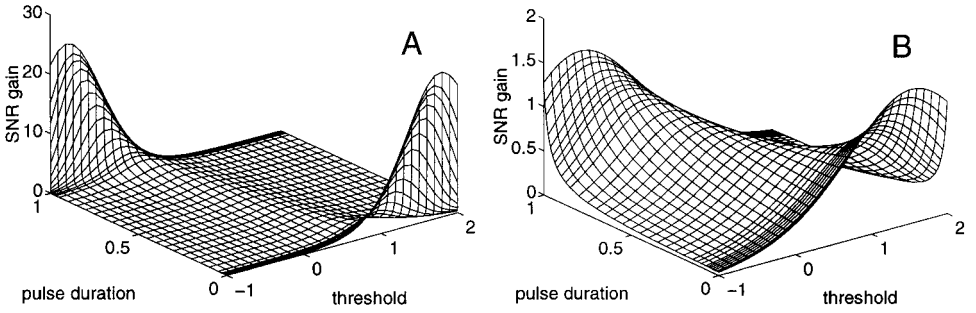

FIG. 6. Input–output SNR gain G_{SNR} from Eq. (12) as a function of the pulse duration T/T_s and the threshold θ, when the input white noise $\eta(t)$ is zero-mean Gaussian with rms amplitude σ_η = 0.4 (panel A) and σ_η = 0.7 (panel B).

conserves the SNR because in the frequency domain both the noise background and the coherent spectral lines are multiplied, in the input–output transformation, by the same value given by the squared modulus of the transfer function of the linear device at this frequency.

At fixed pulse duration T/T_s and noise level σ_η, we find that, thanks to the form of Eqs. (12) and (11), the optimal value of the threshold θ that maximizes the SNR gain G_{SNR} is always the same as the optimal θ maximizing the output SNR R_{out}. For the Gaussian case, this optimal threshold maximizing G_{SNR} is thus given by Fig. 2A, and the corresponding maximum of G_{SNR} appears in Fig. 7.

Figure 7 shows that the maximum SNR gain at the optimal threshold is also found to be larger than unity over a large range of noise levels, especially at small and intermediate noise levels. At high noise levels, the SNR gain saturates slightly below one, indicating that in this case the threshold detector brings no improvement in the SNR. When this detector can be avoided, the SNR at the input is slightly better and, thus, preferable.

At a fixed threshold θ, Eq. (12) allows one to find the optimal value of the

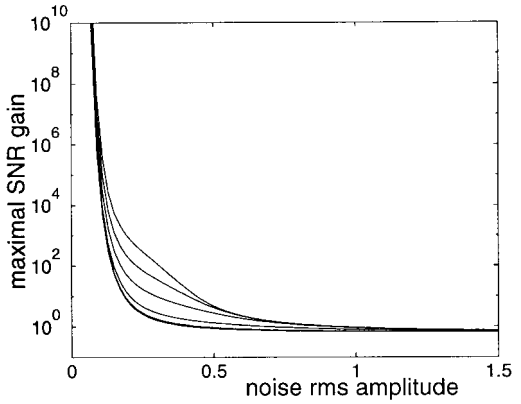

FIG. 7. Maximum input–output SNR gain G_{SNR} from Eq. (12) at the optimal threshold in the conditions of Fig. 2A, with the upper to the lowest curves, $T/T_s = 10^{-6}, 10^{-3}, 10^{-2}$, 0.1, 0.3, and 0.5.

pulse duration T/T_s that maximizes the SNR gain G_{SNR}. For an even density $f_\eta(u)$, the SNR gain verifies $G_{\mathrm{SNR}}(\theta,\ T/T_s = 0) = G_{\mathrm{SNR}}(1-\theta,\ T/T_s = 1)$, and in that case the analysis of Eq. (12) shows that at a fixed $\theta \geq 0.5$ the SNR gain G_{SNR} is maximized when $T/T_s \to 0$. And, symmetrically, at a fixed $\theta \leq 0.5$ the SNR gain G_{SNR} is maximized when $T/T_s \to 1$, as Fig. 6 shows for the Gaussian case.

For two fixed values of the threshold $\theta > 0.5$, Fig. 8a shows the maximum SNR gain G_{SNR} afforded by the optimality condition $T/T_s \to 0$. Strictly, the optimal value $T/T_s = 0$ (or $T/T_s = 1$) cannot be realized because in that case the periodic input $s(t)$ disappears and there is no longer the transmission of a useful signal. In practice, the pulse duration T has to be limited to a nonvanishing value, especially for minimal energy requirements, in order to switch the physical device implementing the threshold detector. For small (near to optimal), but nonvanishing values of T/T_s, Figs. 8b–d also show the resulting SNR gain G_{SNR} and the way it approaches its maximum when $T/T_s \to 0$.

Again, Fig. 8 shows the important property of a SNR gain larger than unity over a large domain of conditions. Also, Fig. 8 shows the second important property, related to the stochastic resonance effect, of the possibility, in various situations with both $\theta > 1$ and $\theta < 1$, of an improvement of the SNR gain by means of noise addition. This form of stochastic resonance is again related to the presence of a threshold that can sometimes be overcome more efficiently by the coherent signal when it receives assistance from the noise.

Equation (12) also shows that, when both the values of the threshold θ and of the pulse duration T/T_s are imposed, so that neither of them can be adjusted to its optimal value, there still exist regimes where the two interesting properties of a SNR gain $G_{\mathrm{SNR}} > 1$ and of $G_{\mathrm{SNR}} > 1$ improvable through noise addition are preserved, as suggested by Figs. 6 and 8. This feature is also illustrated by Fig. 9 which shows, at a fixed pulse duration T/T_s, evolutions of the SNR gain G_{SNR} with the threshold θ and the noise rms amplitude σ_η in the Gaussian case.

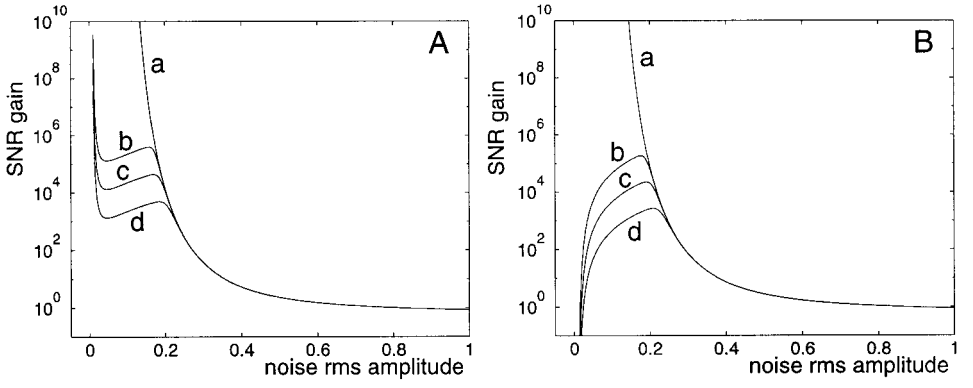

FIG. 8. Input–output SNR gain G_{SNR} from Eq. (12) at a fixed threshold θ for (a) $T/T_s \to 0$, (b) $T/T_s = 10^{-7}$, (c) $T/T_s = 10^{-6}$, (d) $T/T_s = 10^{-5}$. Panel A is for $\theta = 0.95$, and panel B is for $\theta = 1.05$.

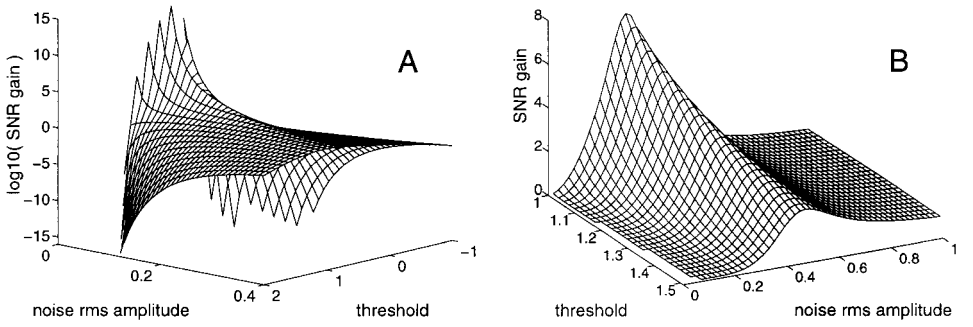

FIG. 9. Input–output SNR gain G_{SNR} of Eq. (12) as a function of the threshold θ and of the rms amplitude σ_η of the zero-mean Gaussian noise $\eta(t)$, at a given pulse duration $T/T_s = 10^{-2}$. Panel A shows the two regimes at $\theta < 1$ and at $\theta > 1$. Panel B is a close-up of the regime at $\theta > 1$, revealing a form of stochastic resonance.

5. THE INFLUENCE OF THE NOISE DISTRIBUTION

The present model, through Eqs. (11) and (12), allows the optimization of the output SNR R_{out} or of the gain G_{SNR} in a similar way for any distribution of the noise $\eta(t)$, other than Gaussian. When the density $f_\eta(u)$ is an even function, its cumulative distribution verifies $F_\eta(-u) = 1 - F_\eta(u)$; as a consequence, in the variables $\theta' = \theta - 0.5$ and $\tau' = T/T_s - 0.5$, the output SNR of Eq. (11) verifies $R_{\mathrm{out}}(\theta', \tau') = R_{\mathrm{out}}(-\theta', -\tau')$ and the SNR gain of Eq. (12) verifies $G_{\mathrm{SNR}}(\theta', \tau') = G_{\mathrm{SNR}}(-\theta', -\tau')$. As a result, both $R_{\mathrm{out}}(\theta, T/T_s)$ and $G_{\mathrm{SNR}}(\theta, T/T_s)$ have a local extremum or saddle point at $(T/T_s, \theta) = (0.5, 0.5)$ which may not, however, be an interesting maximum; this property breaks down when the density ceases to be even.

For illustration of the influence of the noise distribution, Fig. 10 shows typical evolutions of R_{out} as a function of T/T_s and θ. Two distributions have been used for the noise $\eta(t)$ with zero mean and rms amplitude σ_η: a uniform

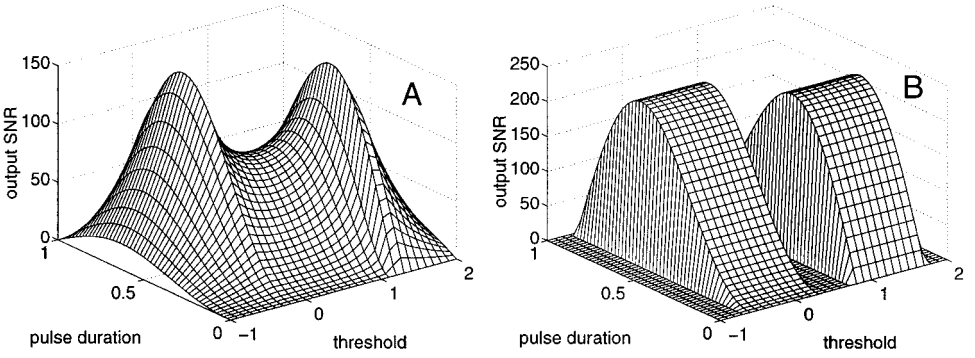

FIG. 10. Output SNR $R_{\mathrm{out}}(1/T_s)$ from Eq. (11) as a function of the pulse duration T/T_s and the threshold θ, when the zero-mean input noise $\eta(t)$ has the rms amplitude $\sigma_\eta = 0.7$ and is uniform (panel A), or dichotomous (panel B). A comparison can be made with the Gaussian distribution of Fig. 1.

distribution over $\eta \in [-\sqrt{3}\sigma_\eta, \sqrt{3}\sigma_\eta]$; and a dichotomous or two-level discrete distribution with $\eta \in \{-\sigma_\eta, \sigma_\eta\}$. The results are comparable to those of Fig. 1 with a Gaussian distribution.

Figure 10 shows that when the noise distribution is changed, one is faced with similar optimization possibilities for maximizing the output SNR R_{out} in various conditions (and the same for maximizing the gain G_{SNR}). For instance, at a fixed noise rms amplitude, there exist optimal values for (T/T_s, θ), both considered as free parameters, that maximize R_{out}. Alternatively, if, for instance, T/T_s is imposed, there is another value of θ that maximizes R_{out}. The optimality conditions maximizing R_{out} are generally different for different noise distributions, but in any situation they can be found through maximization of Eq. (11), and curves similar to those of Figs. 2, 3, 5 could be obtained easily for noises other than Gaussian.

An important point is that the property of stochastic resonance, where R_{out} can be increased through noise addition, is preserved when the noise distribution is changed. This is verified by the results of Fig. 11 in the regime $\theta > 1$, comparable to those of Fig. 4B.

Also, the two interesting properties of a SNR gain $G_{SNR} > 1$ and of $G_{SNR} > 1$ improvable through noise addition, are preserved when the noise distribution is changed, as illustrated by Fig. 12.

Figure 12, comparable to Fig. 9B, illustrates that the optimality conditions maximizing G_{SNR} also differ for differing noise distributions. In Fig. 12 it is shown that with uniform or dichotomous noises the maximum SNR gain at a given $\theta > 1$ increases with increasing θ, whereas it decreases when the noise is Gaussian in Fig. 9B.

If one seeks to maximize the SNR gain G_{SNR} at a fixed pulse duration T/T_s, then one can find, as in Fig. 2A, an optimal value of the threshold θ through maximization of Eq. (12). The resulting maximum of G_{SNR} at the optimal threshold is represented in Fig. 13 with a uniform and a dichotomous noise and is comparable to Fig. 7B with a Gaussain noise.

If we consider the case of the dichotomous noise $\eta(t)$ of Fig. 13B, the behavior

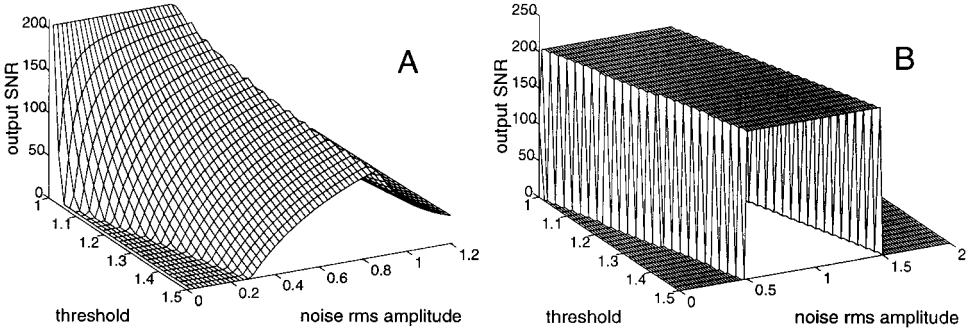

FIG. 11. Output SNR $R_{out}(1/T_s)$ of Eq. (11) as a function of the threshold θ and of the rms amplitude σ_η of the zero-mean noise $\eta(t)$, at a given pulse duration $T/T_s = 0.5$ when $\eta(t)$ is uniform (panel A), or dichotomous (panel B). As is visible, R_{out} can be increased when σ_η increases, revealing a form of stochastic resonance. A comparison can be made with the Gaussian noise of Fig. 4B.

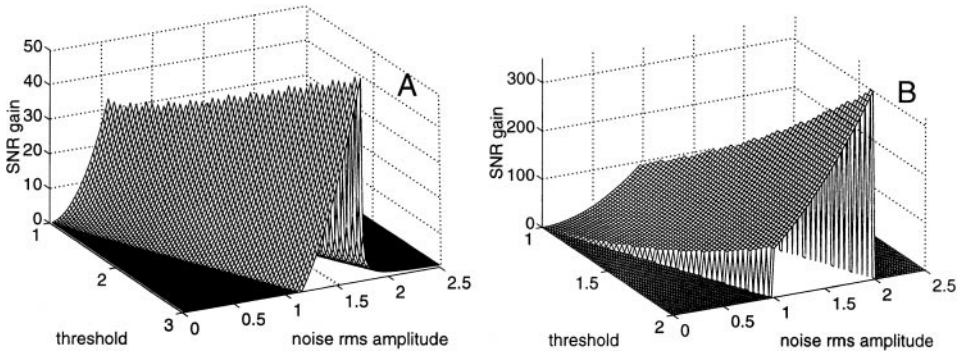

FIG. 12. Input–output SNR gain G_{SNR} of Eq. (12) as a function of the threshold $\theta > 1$ and of the rms amplitude σ_η of the zero-mean noise $\eta(t)$, at a given pulse duration $T/T_s = 10^{-2}$, when $\eta(t)$ is uniform (panel A), or dichotomous (panel B). A comparison can be made with the Gaussian noise of Fig. 9B.

of the detector can be understood with simple threshold-crossing considerations on the input $s(t) + \eta(t)$, and a simple expression can be obtained from Eq. (12) for the maximum of G_{SNR} at the optimal threshold. When $\sigma_\eta < 0.5$, the optimal value of the threshold θ maximizing the output SNR is any value of θ in the interval $]\sigma_\eta,\ 1 - \sigma_\eta[$, which yields an infinite output SNR R_{out} and an infinite SNR gain G_{SNR} since at any $\sigma_\eta > 0$ the input SNR is finite. When $\sigma_\eta > 0.5$, the optimal value of the threshold θ maximizing R_{out} and G_{SNR} is any value of θ verifying $\theta > \sigma_\eta$ and $-\sigma_\eta < \theta - 1 < \sigma_\eta$ which yields, as shown in Fig. 13B, $G_{\mathrm{SNR}} = \sigma_\eta^2/(T/T_s)$ (at least when $T/T_s \leq 0.5$, the other case being recovered by the symmetry properties of $G_{\mathrm{SNR}}(\theta,\ T/T_s)$). The maximum SNR gain $G_{\mathrm{SNR}} = \sigma_\eta^2/(T/T_s)$ is thus an increasing function of the noise rms amplitude σ_η for any $\sigma_\eta > 0.5$.

For similar reasons with the uniform noise of Fig. 13A, when $0 < \sigma_\eta < 0.5/\sqrt{3}$ the maximum gain G_{SNR} is infinite; when $0.5/\sqrt{3} < \sigma_\eta < \sqrt{3}$ the maximum gain

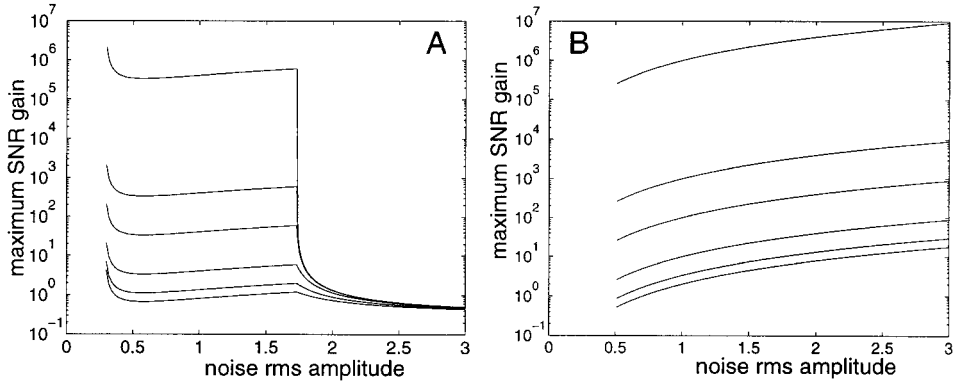

FIG. 13. Maximum input–output SNR gain G_{SNR} from Eq. (12) at the optimal threshold, as a function of the rms amplitude σ_η of the zero-mean noise $\eta(t)$ being uniform (panel A), or dichotomous (panel B). In both panels, from the upper to the lowest curves, $T/T_s = 10^{-6}$, 10^{-3}, 10^{-2}, 0.1, 0.3, and 0.5. A comparison can be made with the Gaussian noise of Fig. 7.

G_{SNR} is finite and increases with increasing σ_η; when $\sigma_\eta > \sqrt{3}$ the maximum G_{SNR} decreases with increasing σ_η. All these evolutions of the gain G_{SNR}, and other properties in more complex situations, are contained in the behavior of Eq. (12) from which they can be deduced by mathematical analysis.

6. DISCUSSION

The present analysis has demonstrated various interesting properties of the simple threshold device of Eq. (1) for the detection of periodic pulse trains.

One interesting property is that this nonlinear detector can act as a SNR amplifier, delivering an output SNR larger than the input SNR. This property can never be obtained with a linear device. In the conditions tested (see Figs. 6–8), the property of a SNR gain $G_{SNR} > 1$ is always present for small to intermediate input noise levels σ_η, and the gain can reach very high values. For large input noise levels σ_η, the SNR gain G_{SNR} saturates to a value slightly below, but very close to, one. Thus, over a large interesting range of conditions the detector behaves as an effective SNR amplifier, and therefore, there is an actual benefit in purposely using the nonlinear detector on the signal-plus-noise mixture, rather than not using it, whenever this choice is available.

When using the detector, if its threshold θ is an adjustable parameter, then it can be set to an optimal value, which depends upon the properties of the input signal-plus-noise mixture (see Fig. 2A, for instance). This optimal value for θ at the same time maximizes the output SNR and the input–output SNR gain. Also, as revealed by the present analysis, there are conditions where the optimal value of the threshold lies above one, i.e. above the amplitude of the coherent pulses to be detected, especially when the input noise level is not too small.

Another remarkable property, when the detector has to operate at a fixed threshold $\theta > 1$, is that there exists an optimal nonzero input noise level that maximizes the output SNR (see Figs. 4 and 11). This means that conditions exist where (purposeful) addition of noise at the input results in an increase of the SNR at the output. This effect is a form of the phenomenon of stochastic resonance, where noise can favor the signal. This is a typically nonlinear effect, which cannot be obtained with linear devices. The same type of improvement through noise addition is also possible for the SNR gain (see Figs. 9 and 12), except that in this case it can even occur when $\theta < 1$, as exemplified by Fig. 8.

Natural systems are known that have to operate in conditions comparable to those considered here. This is the case with neurons, which achieve highly efficient signal processing. At low levels, neurons have to transmit noisy pulse trains in the presence of a fixed neuronal threshold, and it has been shown, both in theoretical models [15] and in experimental situations [16], that they can benefit from noise addition via stochastic resonance. Such nonlinear mechanisms could also benefit technological systems in charge of the transmission of pulse trains, for instance solitons in optical communications.

A comparable study has appeared with another type of stochastic resonant

system in which optimality conditions are sought [17]. Yet with this system of [17] the important property of a SNR gain larger than unity cannot be observed, and the output SNR in [17] is always found to be smaller than the input SNR. In contrast, this important property of $G_{\mathrm{SNR}} > 1$ is available here in our stochastic resonator.

Our present study constitutes a unique analysis, based on an exact theoretical model, of the conditions of optimality for a nonlinear transmission in the presence of stochastic resonance. As such it can serve as a useful basis to extend applications to nonlinear signal processing. The situation of neural systems, that are highly nonlinear at low levels of their constitution with their response threshold, and yet at higher levels achieve very efficient information-processing tasks, also prompts us to envisage the possibilities of novel modalities for signal processing (still to be elucidated), involving devices that would be highly nonlinear as soon as the low levels, and in which stochastic resonance would be a property, among others, contributing to the performance.

REFERENCES

1. Lathi, B. P. *Linear Systems and Signals,* Berkeley–Cambridge Press, Carmichael, CA, (1992).
2. Campbell, D. K., and Ecke, R. E. (Eds.), *Nonlinear Science—The Next Decade,* MIT Press, Cambridge, MA, (1992).
3. Mira, C. Some historical aspects of nonlinear dynamics—Possible trends for the future. *Int. J. Bifurcation Chaos* **7** (1997), 2145–2174.
4. Gammaitoni, L., Hänggi, P., Jung, P., and Marchesoni, F. Stochastic resonance. *Rev. Mod. Phys.* **70** (1998), 223–287.
5. Koch, C., and Segev, I. (editors), *Methods in Neuronal Modeling—From Synapses to Networks,* MIT Press, Cambridge, MA. (1989).
6. Singer, A. C. Signal processing and communication with solitons, in *Digital Signal Processing Handbook* (V. K. Madisetti and D. B. Williams, Eds.), IEEE Press, New York, (1998), pp. 75.1–75.18.
7. Zeitouni, O. On the filtering of noise-contaminated signals observed via hard-limiters, *IEEE Trans. Inf. Theory* **IT-34** (1988), 1041–1048.
8. Chapeau-Blondeau, F. and Godivier, X. Theory of stochastic resonance in signal transmission by static nonlinear systems, *Phys. Rev. E,* **55,** (1997), 1478–1495.
9. Chapeau-Blondeau, F. "Input-output gains for signal in noise in stochastic resonance." *Phys. Lett. A,* **232,** (1997), 41–48.
10. Benzi, R., Sutera, A., and Vulpiani, A. "The mechanism of stochastic resonance." *J. Phys. A,* **14** (1981), L453–L458.
11. Moss, F., Bulsara, A., and Shlesinger, M. F. (editors), "Proceedings NATO Advanced Research Workshop on Stochastic Resonance in Physics and Biology." *J. Statist. Phys.* **70** (1993), 1–512.
12. Wiesenfeld, K., and Moss, F. Stochastic resonance and the benefits of noise: From ice ages to crayfish and SQUIDs, *Nature* **373** (1995), 33–36.
13. Godivier, X., and Chapeau-Blondeau, F. "Noise-assisted signal transmission in a nonlinear electronic comparator: Experiment and theory," *Signal Process.* **56** (1997), 293–303.
14. Godivier, X., Rojas-Varela, J., and Chapeau-Blondeau, F. "Noise-assisted signal transmission via stochastic resonance in a diode nonlinearity," *Electron. Lett.* **33** (1997), 1666–1668.
15. Chapeau-Blondeau, F., Godivier, X., and Chambet, N. "Stochastic resonance in a neuron model that transmits spike trains." *Phys. Rev. E* **53** (1996), 1273–1275.
16. Douglass, J. K., Wilkens, L., Pantazelou, E. and Moss, F. "Noise enhancement of information transfer in crayfish mechanoreceptors by stochastic resonance," *Nature,* **365** (1993), 337–340.
17. Jung, P. "Stochastic resonance and optimal design of threshold detectors," *Physics Letters A,* **207** (1995), 93–104.

FRANÇOIS CHAPEAU-BLONDEAU was born in France in 1959. He received the engineering degree from ESEO, Angers, France, in 1982, the Ph.D. degree in electrical engineering from University Paris VI, France, in 1987, and the *Habilitation* degree from the University of Angers, France, in 1994. In 1988 he was a research associate in the Department of Biophysics at the Mayo Clinic, Rochester, Minnesota, working on biomedical ultrasonics. Since 1990 he has been with the University of Angers, France, as a maitre de conferences. His research interests are in nonlinear signals and systems, including neural systems and discrete-event systems.